Deubiquitylation and stabilization of p21 by USP11 is critical for cell cycle progression and DNA damage responses

Tanggang Deng[1,3], Guobei Yan[1,3], Yu Zhou[1], Xiaoxiao Hu[1], Jianglin Li[1], Jun Hu[1], Hui Zhang[1], Peifu Feng[1], Xunan Sheng[1], Jieying Chen[1], Hongchang Ma[1], Yang Sun[1], Dong Wei, Bin Hu, Jing Liu[2], Weihong Tan[1,*] and Mao Ye[1,*]

[1]Molecular Science and Biomedicine Laboratory, State Key Laboratory for Chemo/Biosensing and Chemometrics, College of Biology, College of Chemistry and Chemical Engineering, Aptamer Engineering Center of Hunan Province, Hunan University, Changsha, Hunan 410082, China

[2]School of Life Sciences, State Key Laboratory of Medical Genetics, Central South University, Changsha, Hunan 410078, China

[3]Co-first author

*Correspondence: Professor Mao Ye or Professor Weihong Tan, College of Biology, Hunan University, 1 Denggao Road, Changsha, Hunan 410082, China. E-mail: yemaocsu@hotmail.com (Mao Ye) or tan@chem.ufl.edu (Weihong Tan).

Abstract

$p21^{WAF1/CIP1}$ is a broad-acting cyclin-dependent kinase inhibitor. Its stability is essential for proper cell cycle progression and cell fate decision. Ubiquitylation by the multiple E3 ubiquitin ligases complex is the major regulatory mechanism of p21, which induces p21 degradation. However, it is unclear whether ubiquitylated p21 can be recycled. In this study, we report that USP11 stabilized p21 by removing the polyubiquitin chains conjugated onto p21. Loss of USP11 promoted p21 degradation and induced the G1/S transition in unperturbed cells. Furthermore, the p21 accumulation mediated by DNA damage was completely abolished in cells depleted of USP11, resulting in the abrogation of the G2 checkpoint. Functionally, the USP11-mediated stabilization of p21 inhibited cell proliferation and tumorigenesis *in vivo*. These findings reveal an important mechanism by which p21 can be stabilized by direct deubiquitylation and pinpoint a critical role of USP11-p21 axis in regulating cell cycle progression and DNA damage responses.

Keywords: p21; ubiquitin; stability; deubiquitylase; cell cycle

Introduction

The cyclin-dependent kinase (CDK) inhibitor p21 (also known as $p21^{WAF1/Cip1}$) is a key negative regulator of cell cycle progression, which mediates cell cycle arrest at the G1 or G2 phase in response to a variety of stress stimuli[1]. p21 contributes to the G1 arrest primarily by inhibiting cyclin E and cyclin A/CDK2 activity[2], which results in the hypo-phosphorylation of the retinoblastoma protein (pRb) and inhibits the release and activation of the transcription factor E2F – a protein required for S-phase entry[3]. p21 sustains cell cycle arrest at the G2 phase by blocking the interaction between CDK1 and CDK-activating kinase, thus inhibiting the activating phosphorylation of CDK1 at Thr-161[4]. Moreover, several studies have reported that p21 also mediates arrest at G2 by retaining the cyclin B1-CDK1 complex in the nucleus, degrading cyclin B and decreasing the expression of early mitotic inhibitor 1 (Emi1)[5, 6, 7].

Under normal growth conditions, p21 is an unstable protein with a relatively short half-life[8, 9]. Its degradation is controlled primarily through ubiquitin-proteasome pathway[9]. Three E3 ubiquitin ligase complexes, SCF^{SKP2}, $CRL4^{CDT2}$ and APC/C^{CDT20}, have been reported to promote p21 ubiquitylation and degradation in the nucleus. During the G1/S transition, the SCF^{SKP2} complex promotes the ubiquitylation and degradation of p21 after it is phosphorylated at Ser130 by CDK2[10, 11], whereas the $CRL4^{CDT2}$ complex mediates the ubiquitin-dependent proteolysis of p21 only when p21 is bound to PCNA and phosphorylated at Ser-114 during the S phase[12]. When bound to CDK1/cyclin B during prometaphase, p21 is degraded by the APC/C^{CDT20} complex[13]. In contrast, p21 stability can be positively regulated by various mechanisms.

Phosphorylation of p21 by p38 alpha, JNK1, AKT and NDR has been reported to enhance its stability[14, 15, 16]. Wisp39, nucleophosmin/B23, hSSB1 and TRIM39 were found to stabilize p21 by engaging in protein-protein interactions[17, 18, 19, 20]. Cables1 stabilizes p21 by antagonizing PSMA3-mediated proteasomal degradation[21]. However, it remains unclear whether p21 can be stabilized by direct deubiquitylation.

The removal of ubiquitin from a target protein by deubiquitylase has emerged as an important regulatory mechanism of many cellular functions. The human genome encodes approximately 98 deubiquitylases that can be subdivided into six families[22]. USP11 is a deubiquitylase that belongs to the ubiquitin-specific processing protease (USP) family, which is primarily localized to the nucleus and possesses multiple highly conserved domains including Cys box, Asp, KRF and His box[23]. Growing evidence has shown that USP11 plays an important role in signal transduction, apoptosis, DNA repair and viral replication by regulating the stability of its substrates[24, 25, 26, 27]. USP11 dysregulation has been found in a variety of tumors, including colorectal cancer, melanoma, glioma and cervical cancer[28, 29, 30].

In this study, we identified USP11 as the first deubiquitylase that directly reverses p21 polyubiquitylation and stabilizes the p21 protein. We also demonstrated that the USP11-p21 axis is critical for regulating cell cycle progression and DNA damage-induced G2 arrest. Our findings fill an important gap of knowledge regarding the regulation of p21 stability and indicate a previously unknown molecular function of USP11 in controlling cell cycle progression.

Results

USP11 interacts with p21

USP11 has been shown to function as a deubiquitylating enzyme that stabilizes multiple cellular proteins by cleaving ubiquitin-protein bonds. To search for cellular proteins that interact with USP11, we expressed Flag-tagged USP11 protein in A549 cells and purified USP11-bound protein complexes using an anti-Flag monoclonal antibody coupled to Dynabeads. USP11-associated proteins were identified by liquid chromatography mass spectrometry/mass spectrometry (LC-MS/MS). Intriguingly, p21 was present in the purified USP11 complexes, but not in the control purifications (Supplementary Fig. 1a). Given the known cellular feature of p21 that can be rapidly degraded by ubiquitylation, we focused our attention on p21 as an interacting protein with USP11.

To confirm the interaction between USP11 and p21, Flag-USP11 or Myc-p21 plasmid was transfected into A549 cells, and co-immunoprecipitations (co-IP) was performed using an anti-Flag or anti-Myc antibody. The results showed that p21was detected in the Flag-USP11 immunoprecipitates (Fig. 1a), and that USP11 was present in Myc-p21 immunoprecipitates (Fig. 1b). Meanwhile, the association of endogenously expressed p21 and USP11 was also investigated using co-IP. USP11 and p21 were separately immunoprecipitated from A549 cells, and the reciprocal protein was detected using western blotting. As shown in Fig. 1c and 1d, both USP11 and p21 were detected in their individual immunoprecipitated complexes, but not in the isotype-matched negative control IgG complexes. To determine whether USP11

and p21 directly interact with each other, we generated and purified recombinant USP11 and p21. Purified GST-USP11 but not the GST control was able to bind to GST-p21 under cell-free conditions (Fig. 1e), demonstrating a direct interaction between USP11 and p21. Similar results were obtained by incubating purified GST-USP11 with extracts from A549 cells (Supplementary Fig. 1b). In addition, the co-localization of both USP11 and p21 occurred in the nucleus (Fig. 1f). Collectively, these results suggest that USP11 physically interacts with p21 *in vivo* and *in vitro*.

To map the USP11-binding region on p21, a series of p21-deletion mutants were expressed in HEK293 cells (Fig. 1g). Co-IP assays revealed that the N-terminal region (aa 1-90) of p21 was critical for the interaction between USP11 and p21 (Fig. 1h). Conversely, mapping the USP11 region required for p21 binding revealed that the C-terminus (aa 536-920) was responsible for the interaction with p21 (Fig. 1i, j).

USP11 influences the steady-state level of p21

Protein-protein interactions are known to play key roles in regulating p21 levels. Given the identified interaction of USP11 with p21, we next investigated whether USP11 affects the steady-state levels of p21. USP11 was introduced into A549 ($p53^{+/+}$) as well as two HCT116 cell lines with a p53 wild-type (HCT116 WT) and null (HCT116 $p53^{-/-}$) genotype. Interestingly, USP11 overexpression resulted in a significant increase of endogenous p21 levels (Fig. 2a), and increasing USP11 expression caused an elevation of p21 levels in a dose-dependent manner in all cell lines regardless of the p53 status (Fig. 2b, c). In contrast, p53 levels were unaffected

by USP11 overexpression, indicating that USP11 increased p21 levels in a p53-independent manner. Notably, overexpression of a catalytically inactive USP11 mutant (C275S/C283S) had no effect on p21 levels (Fig. 2a-c), implying that USP11-mediated upregulation of p21 may depend on the function of USP11 as a deubiquitylating enzyme. To further confirm the regulation of p21, we performed a loss-of-function analysis using two independent USP11-specific short hairpin RNAs (shRNAs) in the above mentioned cell lines. As predicted, USP11 knockdown abolished p21 levels without affecting p53 expression (Fig. 3d). Similar results were obtained using USP11-specific small interfering RNAs (siRNAs) in the A549, H460 and HCT116 cell lines (Supplementary Fig. 2a).

The effect of USP11 on the p21 steady-state levels was not due to changes in transcription because neither USP11 knockdown nor overexpression affected the p21 mRNA levels (Fig. 3e, f; Supplementary Fig. 2b), indicating that USP11 does not regulate p21 expression at the transcriptional level. Furthermore, downregulation of p21 caused by USP11 knockdown could be blocked by the proteasome inhibitor MG132 and Clasto-Lactacystin β-lactone (CLL) (Fig. 3g and Supplementary Fig. 2c), suggesting that USP11 maintains the steady-state level of p21 by blocking its proteasomal degradation.

USP11 stabilizes p21 by deubiquitylation

Because USP11 regulates the steady-state level of p21, we questioned whether USP11 stabilizes p21. To this end, in the presence or absence of Flag-USP11, cells

were treated with cycloheximide (CHX) to inhibit protein biosynthesis, and protein extracts obtained at indicated time points were analyzed. We found that overexpression of wild-type USP11 but not catalytically inactive mutant profoundly extended the half-life of the p21 protein (Fig. 3a, b and Supplementary Fig. 3a). Conversely, knockdown of USP11 resulted in a significant decrease in the half-life of p21 (Fig. 3c and Supplementary Fig. 3b). To further understand the underlying mechanism whereby USP11 regulates the stability of p21, we measured the levels of polyubiquitylation of p21 in HCT116 cells. Silencing USP11 expression using two independent shRNAs led to a significant increase in p21 polyubiquitylation (Fig. 3d), whereas the overexpression of wild-type USP11 reduced the levels of polyubiquitylated p21 (Fig. 3e). In contrast, the catalytically inactive mutant failed to protect p21 from ubiquitylation (Fig. 3e), suggesting that the enzymatic activity of USP11 is essential for the USP11-dependent deubiquitylation of p21. To verify that p21 is a direct substrate of USP11, we purified USP11 and ubiquitylated p21, and incubated these two proteins in a cell-free system. As expected, wild-type USP11 but not the catalytically inactive mutant decreased p21 polyubiquitylation in vitro (Fig. 3f). These data indicate that USP11 directly deubiquitylates p21.

To investigate the type of poly-Ub chain on p21 that is removed by USP11, we transfected HCT116 cells with Myc-tagged p21, together with HA-tagged ubiquitin mutants in which all lysines, except only one lysine (K6, K11, K27, K29, K33, K48 or k63), were mutated into arginines. As shown in Fig. 3g, USP11 knockdown significantly increased K48-linked poly-Ub but not any other isopeptide-linked (K6,

K11, K27, K29, K33 or K63) poly-Ub. The result suggests that USP11 removes K48-linked poly-Ub from p21.

USP11 knockdown abolishes p21 elevation triggered by genotoxic agents.

p21 can be induced under DNA damage condition via p53-dependent and p53-independent pathways. To explore whether USP11 is involved in the DNA damage-mediated regulation of p21, we treated cells with genotoxic agents. In agreement with previous reports, etoposide treatment led to the upregulation of p21 levels in HCT116 WT and HCT116 $p53^{-/-}$ cells (Fig. 4a). Intriguingly, etoposide-induced p21 accumulation was significantly abolished in USP11-depleted cells (Fig. 4a). Similarly, USP11 knockdown also significantly decreased the p21 elevation triggered by doxorubicin (Fig. 4b). Notably, depletion of USP11 did not abolish the induction of p21 mRNA in response to genotoxic treatment (Fig. 4c, d). Collectively, these findings suggest that USP11 is indispensable for the expression of p21 under physiological conditions as well as in response to DNA damage (Fig. 4e).

USP11 revers p21 polyubiquitylation in a cell cycle-independent manner

Three E3 ubiquitin ligase complexes, SCF^{SKP2}, $CRL4^{CDT2}$ and APC/C^{CDC20}, have been reported to induce p21 ubiquitylation and degradation at different phases during an unperturbed cell cycle. To assess which E3 ubiquitin ligase complex is regulated by USP11, HCT116 cells stably expressing the indicated shRNAs were synchronized at each phase (Supplementary Fig. 4). Strikingly, USP11 knockdown led to a

significant decrease of p21 at all phases of the cell cycle, although the p21 protein level varied during the cell cycle (Fig. 5a). Furthermore, we examined whether the effect of USP11 on p21 was associated with SCF^{SKP2}, $CRL4^{CDT2}$ or APC/C^{CDC20}. Knockdown of USP11 using shRNAs significantly decreased p21 levels with concomitant increases in SKP2, but the levels of CDT2 and CDC20 were unchanged (Fig. 5b-c). However, when SKP2, CDT2 or CDC20 was knocked down by siRNA, USP11 depletion-induced p21 degradation and ubiquitylation was abolished (Fig. 5b-g). Altogether, these results indicate that USP11 stabilizes p21 via the reversal of SCF^{SKP2}, $CRL4^{CDT2}$ or APC/C^{CDC20}-mediated ubiquitylation and degradation in a cell cycle-independent manner (Fig. 5h).

USP11 regulates cell cycle progression and the DNA damage response in a p21-dependent manner

Because p21 regulates cell cycle progression at G1 phase, we hypothesized that USP11 may affect cell cycle progression from G1 to S phase. To test this hypothesis, the percentage of cells in S phase was determined by measuring the DNA content and incorporation of BrdU, as well as by performing double thymidine block and release. As predicted, the percentage of cells in S phase was increased when USP11 was knocked down in HCT WT and HCT116 $p53^{-/-}$ cells (Fig. 6a-c; Supplementary Fig5a, 6a). In contrast, USP11 depletion in HCT116 $p21^{-/-}$ cells exhibited no effects on the G1/S transition (Fig. 6a, b; Supplementary Fig. 5a), but USP11-depleted cells transfected with exogenous p21 fully prevented the G1/S transition induced by

USP11 ablation (Fig. 6d). These results strongly suggest that the USP11-mediated G1/S transition is dependent on p21.

To determine whether p21 is required for the function of USP11 in the G2/M checkpoint after DNA damage, cells were treated with a low-dose of doxorubicin. The phopho-histone3 (pH3) at Ser10, an indicator of cells at M phase, was used to monitor the G2/M checkpoint. As shown in Fig. 6e, after doxorubicin treatment, the percentage of cells in M phases was significantly increased in HCT WT cells with USP11 knockdown. However, in HCT116 cells lacking p21 (HCT116 $p21^{-/-}$), silencing USP11 had no effect on the increased percentage of cells in M phase, indicating that USP11 depends on p21 to sustain the DNA damage-induced G2/M checkpoint (Fig. 6e; Supplementary Fig. 6b).

To investigate the effect of USP11 on apoptosis induced by a DNA-damaging agent, HCT116 WT and HCT116 $p21^{-/-}$ cells were treated with either doxorubicin or etoposide. The percentage of cells in sub-G1 phase (apoptotic cells) was measured using flow cytometry with propidium iodide staining. Compared with the control cells, USP11-depleted HCT116 WT cells exhibited a significant increase in the levels of apoptosis after a 24-h treatment with either doxorubicin or etoposide (Figure 6f, g). Interestingly, USP11 knockdown did not affect apoptosis triggered by either doxorubicin or etoposide in cells lacking p21 (Fig.6g). Collectively, these data show that USP11 knockdown sensitizes cells to DNA damage-induced apoptosis by abolishing p21 accumulation.

Loss of USP11 promotes tumor cell growth via the downregulation of p21

To investigate whether USP11 functions as a tumor suppressor by regulating p21, USP11-depleted A549 cells were implanted into nude mice and tumor growth was monitored at the indicated time points. Compared with mice implanted with control shRNA-infected cells, mice bearing USP11-shRNA expressing A549 cells showed increased tumor growth throughout the experiment (Fig. 7a). At 37 days after tumor cell implantation, the volume and weight of the tumor formed by USP11-depleted A549 cells were significantly increased. (Fig. 7a-c). The results of an immunohistochemical analysis verified the reduced expression of USP11 and p21 in the xenograft tumors (Fig. 7d). Next, we analyzed the effect of USP11 on cell proliferation. We found that USP11 depletion promoted the proliferation of A549 and HCT116 WT cells, and that p21 restoration completely reversed the effect of USP11 depletion (Fig. 7e). Notably, USP11 knockdown showed no effect on the proliferation of HCT116 $p21^{-/-}$ cells (Fig.7e). Conversely, overexpression of USP11, but not the catalytically inactive mutant of USP11, inhibited the proliferation of A549 and HCT116 WT cells (Fig. 7f). Similarly, overexpression of USP11 had no effect on the proliferation of HCT116 $p21^{-/-}$ cells (Fig. 7f). Therefore, the loss of USP11 results in increased proliferation of tumor cells via the downregulation of p21.

Discussion

In the present study, we identified USP11 as a p21 deubiquitylase. Our results indicate that USP11 and p21 interact with each other and colocalize in the nucleus. Overexpression of USP11 stabilizes p21 by removing its ubiquitin chain, whereas USP11 downregulation decreases p21 levels, which is accompanied by increasing ubiquitylation. To the best of our knowledge, this is the first evidence that p21 can be stabilized by direct deubiquitylation mediated by a deubiquitylase.

p21 is a well-known transcriptional target of p53. In response to various stresses including DNA damage and oxidative stress, activation of p53 induces p21 protein expression by binding its promoter[31]. A recent study revealed that USP11 deubiquitylates and stabilizes p53[32]. However, our results indicated that USP11 had no effect on p53. USP11 overexpression or knockdown failed to affect p53 levels, which is consistent with a previous study demonstrating that USP11 does not interact with p53 and exhibit any effect on the levels of p53 ubiquitylation or stabilizing p53[33]. Furthermore, we found USP11 exerts its function on p21 both in p53 wild-type and null cell lines, suggesting that USP11 regulates p21 levels in a p53-independent manner. In response to genotoxic treatment, p21 was accumulated in p53 wild-type and null cell lines. Strikingly, USP11 knockdown completely abolished p21 elevation induced by genotoxic agents, but not p21 mRNA induction. This finding reveals the interesting fact that the stability of p21 mediated by USP11 is indispensable for both p53-dependent and p53-independent transactivation of p21.

p21 is an unstable protein with a relatively short half-life that can respond to rapid

intrinsic and extrinsic alterations[9]. Its stability is regulated mainly by post-translational modifications such as phosphorylation and ubiquitylation[34]. For the ubiquitin-dependent pathway, three E3 ubiquitin ligase complex, SCF^{SKP2}, $CRL4^{CDT2}$ and APC/C^{CDT20}, have been identified to promote p21 ubiquitylation and degradation at specific stages of the cell cycle. SCF^{SKP2} is necessary for p21 degradation at the G1/S transition as well as during S phase of the cell cycle [35], whereas $CRL4^{CDT2}$ specifically targets p21 for degradation in S phase [36]. During mitosis, the APC/C^{CDT20} complex primarily drives p21 degradation [13]. Here, we showed that USP11 protected p21 from ubiquitin-mediated degradation by abolishing the action of the above E3 ubiquitin ligase complex. Loss of p21 expression upon USP11 knockdown was significantly ameliorated by depleting SKP2, CDT2 and CDC20, indicating that USP11-mediated protection of p21 is independent of the cell cycle. Notably, knocking down USP11 caused a significant increase of SKP2 levels without affecting either CDT2 or CDC20 expression. Given that the change in SKP2 levels coincides with the functional activity of USP11 with regard to p21 stability, we speculated that SKP2 may contribute to a positive feedback regulation that enhances the effects of USP11 on p21, but the detailed mechanism underlying USP11-dependent regulation of SKP2 remains to be elucidated.

p21 plays a critical role in cell cycle progression and the cellular response to DNA damage by arresting cell cycle progression at the G1/S and G2/M transitions. Consistent with this notion, our results showed that USP11 depletion promoted the G1/S transition in unperturbed cells, which could be reversed by the ectopic expression of p21. Similar results were obtained in HCT116 $p53^{-/-}$ cells, which is consistent with the result that

USP11 regulates the protein levels of p21 in a p53-independent manner. In response to DNA damage, USP11 knockdown abrogates the G2/M checkpoint in cells exposed to genotoxic treatment, which promotes mitotic entry and induces apoptosis. Notably, USP11 knockdown in HCT116 $p21^{-/-}$ cells had no effect on the G1/S transition or DNA damage-induced G2/M checkpoint, suggesting that USP11 is involved in regulating the cell cycle through p21. Collectively, these findings indicated that the USP11-p21 axis plays an important role in regulating cell cycle progression and DNA damage-induced G2 arrest.

It has been reported that p21 can function as a tumor suppressor as well as an oncogene. This dual behavior of p21 primarily depends on its subcellular location. The tumor-suppressive activities of p21 are associated with its nuclear localization, whereas cytoplasmic p21 contributes to its oncogenic effects[9, 37, 38]. Our results show that USP11 acts as tumor suppressor, as overexpression of USP11 inhibited cell proliferation, whereas cells with USP11 depletion exhibited increased proliferation. This is consistent with previous reports that USP11 functions as a tumor suppressor [30, 39, 40]. Furthermore, silencing USP11 in HCT116 $p21^{-/-}$ cells had no effect on the proliferation, indicating that USP11 exerts its function via p21. Given that USP11 interacts with p21 in the nucleus, we speculated that the biological function of USP11 is associated with the tumor-suppressive activities of nuclear p21. Further studies are necessary to establish a detailed association between USP11 and a variety of human cancers, which will provide clue as to how to utilize USP11 as a potential cancer therapeutic target.

Methods

Cell culture and reagents

HEK293 cells were cultured in DMEM (GIBCO cat. 8116490) supplemented with 10% (vol/vol) FBS; A549 cells were cultured in RPMI 1640 (GIBCO cat. 8116491) supplemented with 10% FBS and HCT116 WT, HCT116 $p53^{-/-}$, and HCT116 $p21^{-/-}$ cells were cultured in McCoy's 5A medium (Invitrogen cat. 16600082) supplemented with 10% FBS. The following reagents were used: MG132 (Sigma cat. C2211-5MG), nocodazole (Sigma cat. M1404-10MG), GSH-Sepharose (Thermo Fisher Scientific cat. 16100), doxorubicin (Sigma cat. D1515-10MG), and etoposide (Sigma cat. E1383-25MG).

Plasmids

Full-length USP11 was PCR-amplified from human cDNA and subcloned into the pCMV-Tag2B vector (containing a Flag tag) to create a Flag-tagged USP11 expression plasmid. Various USP11 deletion mutants were generated using PCR. GST-USP11 was constructed by inserting USP11 cDNA into the pGEX-4T-1 vector. GST-p21, myc-p21, and various p21 deletion mutants with an HA tag were gifts from Tiebang Kang. All the constructs were sequenced prior to use.

Antibodies

Anti-p53 (DO-1, cat. sc-126), anti-CDC20 (E7, cat. sc-13162) anti-USP11 (cat. sc-365528) and anti-MDM2 (cat. sc-965) antibodies were purchased from Santa Cruz. Anti-p21 (BD Pharmingen cat. 556430/Cell Signaling Technology cat. #2947). Anti-USP11 (A301-613A) and anti-CDT2 (cat. A300-947A) antibodies were purchased from

Bethyl Laboratories. Anti-histone H3 (phospho-S10) antibodies (cat. ab5176) were purchased from Abcam. Anti-Flag (cat. M185-3L), anti-Myc (cat. M192-3) and anti-HA (cat. M180-3) antibodies were purchased from Medical & Biological Laboratories Co., Ltd. Anti-GAPDH (cat. KC-5G4) antibodies were purchased from Kangchen Bio-tech.

Immunofluorescence staining

Cells were cultured in Lab-Tek chambers for 24 h, washed three times with phosphate-buffered saline (PBS), and fixed with 4% paraformaldehyde for 15 min. The fixed cells were then washed twice with PBS, permeabilized for 10 min with 0.2% Triton X-100, blocked for 1 h in 5% BSA and incubated with the appropriate primary antibodies overnight at 4°C. The USP11 (1:200) and p21 (1:200) antibodies were used to detect endogenous protein expression. Cells were labeled for 1 h using secondary antibodies conjugated to either FITC (Thermo Fisher Scientific cat. 20-58-060111) or Texas Red (Thermo Fisher Scientific cat. 19-183-062312) at room temperature followed by three washes with PBS. Cells were then counterstained with DAPI at room temperature for 5 min to visualize nuclear DNA. Fluorescence images were acquired using a confocal microscope (Zeiss LSM510).

Western blotting and immunoprecipitation

Western blotting and co-IP were performed as described previously. Briefly, cells were lysed in M-PER buffer (Thermo Fisher Scientific cat. 78501) containing protease inhibitors (Biotool cat. B14001), and the clarified lysates were resolved on 12% gels using SDS-PAGE and transferred to nitrocellulose membranes for western blotting

using ECL detection reagents (Advansta cat. 160625-66). Alternatively, 3 mg of clarified lysates was incubated overnight at 4°C with 3 μg of either relevant primary antibodies or an isotype-matched negative control IgG. Subsequently, the samples were incubated for 1 h with 30 μl of magnetic beads conjugated with protein G (Invitrogen cat.10004D) and then washed four times with co-IP/wash buffer. Precipitated proteins were dissolved in 2× SDS sample buffer, boiled, and subjected to western blot analysis.

GST pulldown assays

Bacterially expressed GST-USP11 was retained on glutathione sepharose beads (Promega cat.V8611) and incubated for 1 h at 4°C with A549 cells extracts.

Protein half-life assays

Cells were treated with cycloheximide (50 μg ml^{-1}) for various periods of time to block protein synthesis. Crude extracts were prepared, and the protein levels were assessed using western blot analysis.

Synchronization of HCT116 WT cells

To synchronize HCT116 WT cells at the G1/S border, cells were treated with 2 mM thymidine (Millipore cat. 6060-5mg) for 18 h. Cells were released from the block by washing with PBS followed by the addition of complete growth medium. After 9 h, thymidine was added to the medium to a final concentration of 2 mM, and the cells were cultured for an additional 18 h. Cells were then rinsed twice with PBS, cultured in complete growth medium for 3 h (S-phase cells), 6 h (G2-phase cells) or treated with culture media containing 100 ng ml^{-1} of nocodazole for 11 h (M-phase cells). Cells were collected and analyzed using flow cytometry and western blotting.

Real-time PCR

Total RNA was extracted using Eastep® (Promega cat.LS1040). RNA (1 μg) was reverse transcribed in a 20μL reaction using a FastQuant RT Super Mix Kit (TIANGEN cat. KR106-02). After reverse transcribing the RNA at 42°C for 15 min followed by inactivation of the polymerase at 95°C for 3 min, the RT reaction was diluted. The resulting cDNA was used for real-time PCR (RT-PCR) using the following primer sequences:

USP11-F	AGGTGTCAGGTCGCATTGAG
USP11-R	TGAGAGCCGGTACATCAGGA
GAPDH-F	AAGGTGAAGGTCGGAGTCAA
GAPDH-R	AATGAAGGGGTCATTGATGG
p53-F	GCTTTCCACGACGGTGAC
p53-R	GCTCGACGCTAGGATCTGAC
p21-F	ATTAGCAGCGGAACAAGGAGTCAGACAT
p21-R	CTGTGAAAGACACAGAACAGTACAGGGT

RNA interference and lentivirus transduction

The sequences of the USP11 siRNAs have been previously reported (siUSP11#1: 5'-AATGAGAATCAGATCGAGTCC-3'; siUSP11#2: 5'-AAGGCAGCCTATGTCCTCTTC-3'), and the sequence of the control siRNA is 5'-TTCTCCGAACGTGTCACGTTTC-3' (all synthesized by Shanghai GenePharma). siRNA transfection was performed according to the manufacturer's protocol. After 48 h, the cells were washed with PBS and lysed directly into M-PER lysis buffer, after

which the protein levels were assessed by western blot analysis. To stably knock down endogenous USP11 expression, we used a lentiviral packaging shRNA expression vector (purchased from GenePharma, Shanghai, China) to transduce the cells. Target cells were infected with lentivirus for 24-48 h according to manufacturer's instructions. The following shRNA target sequences were used: shUSP11#1, 5'-CCGTGATGATATCTTCGTCTA-3'; shUSP11#2, 5'-AAGGCAGCCTATGTCCTCTTC-3'; and non-targeting control, 5'-TTCTCCGAACGTGTCACGT-3'.

***In vivo* ubiquitylation assay**

HCT116 WT cells were infected with the indicated lentiviruses followed by treatment with 20 μM MG132 for 6 h, washes with PBS, and lysis in M-PER buffer containing protease inhibitors. The lysates were centrifuged to obtain the cytosolic protein fraction, which was incubated with anti-p21 antibodies overnight followed by protein A/G agarose beads for an additional 1 h at room temperature. Then, the beads were washed three times with wash buffer. The proteins were released from the beads by boiling the beads in SDS-PAGE sample buffer, and they were analyzed using immunoblotting with anti-HA monoclonal antibodies.

***In vitro* ubiquitylation of p21**

To prepare p21 as the substrate for the *in vitro* deubiquitylation assay, HCT116 WT cells were transfected with Myc-p21 with or without co-transfected HA-ubiquitin and treated with 20 μM MG132 for 6 h. Non-ubiquitylated or ubiquitylated Myc-p21 was purified from the cell extracts using an anti-Myc antibody. Either GST-tagged USP11

or the GST-tagged USP11^{mut} was expressed in the BL21 *Escherichia coli* strain. After the cells were induced with 0.4 mM IPTG, they were lysed, and GST-USP11 was purified using glutathione agarose (Pierce®, Thermo Fisher cat.16100) and eluted with elution buffer (50 mM Tris, 150 mM NaCl, pH 8.0) containing 10 mM deduced glutathione (Sigma cat.G4251). Non-ubiquitylated or ubiquitylated Myc-p21 was incubated with purified USP11 in deubiquitylation buffer (50 mM Tris-HCl (pH 8.0), 50 mM NaCl, 1 mM EDTA, 10 mM dithiothreitol and 5% glycerol) for 2 h at 37°C.

BrdU labeling

Cells stably expressing the indicated shRNAs for 48 h were washed twice with PBS and incubated with 20 μM BrdU for 1 h, after which they were prepared for flow cytometry according to the manufacturer's protocol (BD Biosciences cat.559619).

G2/M checkpoint assay

Cells stably expressing the indicated shRNAs were pretreated with 0.2 μM doxorubicin for 2 h, synchronized with nocodazole (100 ng ml^{-1}) for 16 h, harvested and then fixed with 70% ethanol at -20°C. Thereafter, the cells were resuspended in 1 ml of 0.25% Triton X-100 in PBS and incubated at 4°C for 15 min with gentle rocking. After the cells were centrifuged, the cell pellet was resuspended in 200 μl of PBS containing 1% BSA and 1.5 μg of a polyclonal antibody that specifically recognizes the phosphorylated form of histone H3 (Abcam) and incubated for 1.5 h at room temperature. The cells were then rinsed with PBS containing 1% BSA and incubated with a fluorescein isothiocyanate (FITC)-conjugated goat anti-rabbit antibody (CMCTAG cat.AT0118) diluted at a ratio of 1:50 in PBS containing 1% BSA. After a

30-min incubation at room temperature in the dark, the cells were stained with propidium iodide, and cellular fluorescence was measured using flow cytometry.

Cell proliferation assay

A549, HCT116 WT and HCT116 $p21^{-/-}$ cells that were infected with the indicated lentiviral shRNA constructs for at least 48 h were seeded into 6-well plates at an optimized density of 3×10^5 cells per well. Then, p21 was transfected into the indicated cells for an additional 24 h. Cells were then seeded into a 96-well plate at an optimized density of 8×10^3 cells per well. At the indicated time points, a 3-(4,5-dimethylthiazol-2-yl)-2,5-diphenyltetrazolium bromide solution (Beyotime Biotechnology, China cat.ST316) was added to each well and incubated at 37°C for 4 h. The supernatants were aspirated carefully, and 100 μl of DMSO was added. The absorbance of the individual wells was determined at 490 nm. Each condition was conducted in quadruplicate, and the experiment was repeated at least three times.

***In vivo* tumorigenesis study.**

To establish lung cancer xenografts in nude mice, a total of 5×10^6 A549 cells in the logarithmic growth phase that were stably transfected with either control or the indicated shRNAs targeting USP11 were harvested, washed twice with PBS, suspended in 100 μl of PBS and injected into the right flank of each mouse (n=5 per group). The tumor size was measured every two days for 37 days using a caliper, and the tumor volume was calculated based on the following formula: $V=0.5\ (\text{length}\times\text{width}^2)$.

References

1. Niculescu AB, 3rd, Chen X, Smeets M, Hengst L, Prives C, Reed SI. Effects of p21(Cip1/Waf1) at both the G1/S and the G2/M cell cycle transitions: pRb is a critical determinant in blocking DNA replication and in preventing endoreduplication. *Mol Cell Biol* **18**, 629-643 (1998).
2. Brugarolas J, Moberg K, Boyd SD, Taya Y, Jacks T, Lees JA. Inhibition of cyclin-dependent kinase 2 by p21 is necessary for retinoblastoma protein-mediated G1 arrest after gamma-irradiation. *Proc Natl Acad Sci U S A* **96**, 1002-1007 (1999).
3. Ewen ME, Sluss HK, Sherr CJ, Matsushime H, Kato J, Livingston DM. Functional interactions of the retinoblastoma protein with mammalian D-type cyclins. *Cell* **73**, 487-497 (1993).
4. Smits VA, Klompmaker R, Vallenius T, Rijksen G, Makela TP, Medema RH. p21 inhibits Thr161 phosphorylation of Cdc2 to enforce the G2 DNA damage checkpoint. *J Biol Chem* **275**, 30638-30643 (2000).
5. Charrier-Savournin FB, Chateau MT, Gire V, Sedivy J, Piette J, Dulic V. p21-Mediated nuclear retention of cyclin B1-Cdk1 in response to genotoxic stress. *Mol Biol Cell* **15**, 3965-3976 (2004).
6. Gillis LD, Leidal AM, Hill R, Lee PW. p21Cip1/WAF1 mediates cyclin B1 degradation in response to DNA damage. *Cell Cycle* **8**, 253-256 (2009).
7. Lee J, Kim JA, Barbier V, Fotedar A, Fotedar R. DNA damage triggers p21WAF1-dependent Emi1 down-regulation that maintains G2 arrest. *Mol Biol Cell* **20**, 1891-1902 (2009).

8. Blagosklonny MV, Wu GS, Omura S, el-Deiry WS. Proteasome-dependent regulation of p21WAF1/CIP1 expression. *Biochem Biophys Res Commun* **227**, 564-569 (1996).

9. Warfel NA, El-Deiry WS. p21WAF1 and tumourigenesis: 20 years after. *Curr Opin Oncol* **25**, 52-58 (2013).

10. Wang W, Nacusi L, Sheaff RJ, Liu X. Ubiquitination of p21Cip1/WAF1 by SCFSkp2: substrate requirement and ubiquitination site selection. *Biochemistry* **44**, 14553-14564 (2005).

11. Yu ZK, Gervais JL, Zhang H. Human CUL-1 associates with the SKP1/SKP2 complex and regulates p21(CIP1/WAF1) and cyclin D proteins. *Proc Natl Acad Sci U S A* **95**, 11324-11329 (1998).

12. Abbas T, Sivaprasad U, Terai K, Amador V, Pagano M, Dutta A. PCNA-dependent regulation of p21 ubiquitylation and degradation via the CRL4Cdt2 ubiquitin ligase complex. *Genes Dev* **22**, 2496-2506 (2008).

13. Amador V, Ge S, Santamaria PG, Guardavaccaro D, Pagano M. APC/C(Cdc20) controls the ubiquitin-mediated degradation of p21 in prometaphase. *Mol Cell* **27**, 462-473 (2007).

14. Kim GY, Mercer SE, Ewton DZ, Yan Z, Jin K, Friedman E. The stress-activated protein kinases p38 alpha and JNK1 stabilize p21(Cip1) by phosphorylation. *J Biol Chem* **277**, 29792-29802 (2002).

15. Li Y, Dowbenko D, Lasky LA. AKT/PKB phosphorylation of p21Cip/WAF1 enhances protein stability of p21Cip/WAF1 and promotes cell survival. *J Biol Chem*

277, 11352-11361 (2002).

16. Cornils H, Kohler RS, Hergovich A, Hemmings BA. Human NDR kinases control G(1)/S cell cycle transition by directly regulating p21 stability. *Mol Cell Biol* **31**, 1382-1395 (2011).
17. Benzeno S, Diehl JA. A novel WISp39 protein links Hsp90 and p21 stability to the G2/M checkpoint. *Cancer Biol Ther* **4**, 376-378 (2005).
18. Xiao J*, et al.* Nucleophosmin/B23 interacts with p21WAF1/CIP1 and contributes to its stability. *Cell Cycle* **8**, 889-895 (2009).
19. Xu S*, et al.* hSSB1 binds and protects p21 from ubiquitin-mediated degradation and positively correlates with p21 in human hepatocellular carcinomas. *Oncogene* **30**, 2219-2229 (2011).
20. Zhang L*, et al.* TRIM39 regulates cell cycle progression and DNA damage responses via stabilizing p21. *Proc Natl Acad Sci U S A* **109**, 20937-20942 (2012).
21. Shi Z*, et al.* Cables1 controls p21/Cip1 protein stability by antagonizing proteasome subunit alpha type 3. *Oncogene* **34**, 2538-2545 (2015).
22. Fraile JM, Quesada V, Rodriguez D, Freije JM, Lopez-Otin C. Deubiquitinases in cancer: new functions and therapeutic options. *Oncogene* **31**, 2373-2388 (2012).
23. Ideguchi H*, et al.* Structural and functional characterization of the USP11 deubiquitinating enzyme, which interacts with the RanGTP-associated protein RanBPM. *Biochem J* **367**, 87-95 (2002).
24. Sun W*, et al.* USP11 negatively regulates TNFalpha-induced NF-kappaB activation by targeting on IkappaBalpha. *Cell Signal* **22**, 386-394 (2010).

25. Wiltshire TD, Lovejoy CA, Wang T, Xia F, O'Connor MJ, Cortez D. Sensitivity to poly(ADP-ribose) polymerase (PARP) inhibition identifies ubiquitin-specific peptidase 11 (USP11) as a regulator of DNA double-strand break repair. *J Biol Chem* **285**, 14565-14571 (2010).

26. Liao TL, Wu CY, Su WC, Jeng KS, Lai MM. Ubiquitination and deubiquitination of NP protein regulates influenza A virus RNA replication. *EMBO J* **29**, 3879-3890 (2010).

27. Xu Z, *et al.* USP11, Deubiquitinating Enzyme, Associated with Neuronal Apoptosis Following Intracerebral Hemorrhage. *J Mol Neurosci* **58**, 16-27 (2016).

28. Lee EW, Seong D, Seo J, Jeong M, Lee HK, Song J. USP11-dependent selective cIAP2 deubiquitylation and stabilization determine sensitivity to Smac mimetics. *Cell Death Differ* **22**, 1463-1476 (2015).

29. Lin CH, Chang HS, Yu WC. USP11 stabilizes HPV-16E7 and further modulates the E7 biological activity. *J Biol Chem* **283**, 15681-15688 (2008).

30. Wu HC, *et al.* USP11 regulates PML stability to control Notch-induced malignancy in brain tumours. *Nat Commun* **5**, 3214 (2014).

31. Jung YS, Qian Y, Chen X. Examination of the expanding pathways for the regulation of p21 expression and activity. *Cell Signal* **22**, 1003-1012 (2010).

32. Ke JY, *et al.* USP11 regulates p53 stability by deubiquitinating p53. *J Zhejiang Univ Sci B* **15**, 1032-1038 (2014).

33. Li M, *et al.* Deubiquitination of p53 by HAUSP is an important pathway for p53 stabilization. *Nature* **416**, 648-653 (2002).

34. Abbas T, Dutta A. p21 in cancer: intricate networks and multiple activities. *Nat Rev Cancer* **9**, 400-414 (2009).

35. Frescas D, Pagano M. Deregulated proteolysis by the F-box proteins SKP2 and beta-TrCP: tipping the scales of cancer. *Nat Rev Cancer* **8**, 438-449 (2008).

36. Abbas T, Dutta A. CRL4Cdt2: master coordinator of cell cycle progression and genome stability. *Cell Cycle* **10**, 241-249 (2011).

37. Kreis NN, Louwen F, Yuan J. Less understood issues: p21(Cip1) in mitosis and its therapeutic potential. *Oncogene* **34**, 1758-1767 (2015).

38. Romanov VS, Rudolph KL. p21 shapes cancer evolution. *Nat Cell Biol* **18**, 722-724 (2016).

39. Lim KH, Suresh B, Park JH, Kim YS, Ramakrishna S, Baek KH. Ubiquitin-specific protease 11 functions as a tumor suppressor by modulating Mgl-1 protein to regulate cancer cell growth. *Oncotarget* **7**, 14441-14457 (2016).

40. Zhang E*, et al.* Ubiquitin-specific protease 11 (USP11) functions as a tumor suppressor through deubiquitinating and stabilizing VGLL4 protein. *Am J Cancer Res* **6**, 2901-2909 (2016).

Acknowledgments

We would like to thank Han You for generously providing the HCT116 $p21^{-/-}$ and HCT116 $p53^{-/-}$ cells. This work was supported by grants from the National Basic Research Program of China (No. 2013CB932702), the National Natural Science Foundation of China (Nos. 81171950, 81272220, 81402304 and 81672760), the

Interdisciplinary Research Program of Hunan University and the Program for New Century Excellent Talents in University (NCET-13-0195).

Figures and Figure Legends

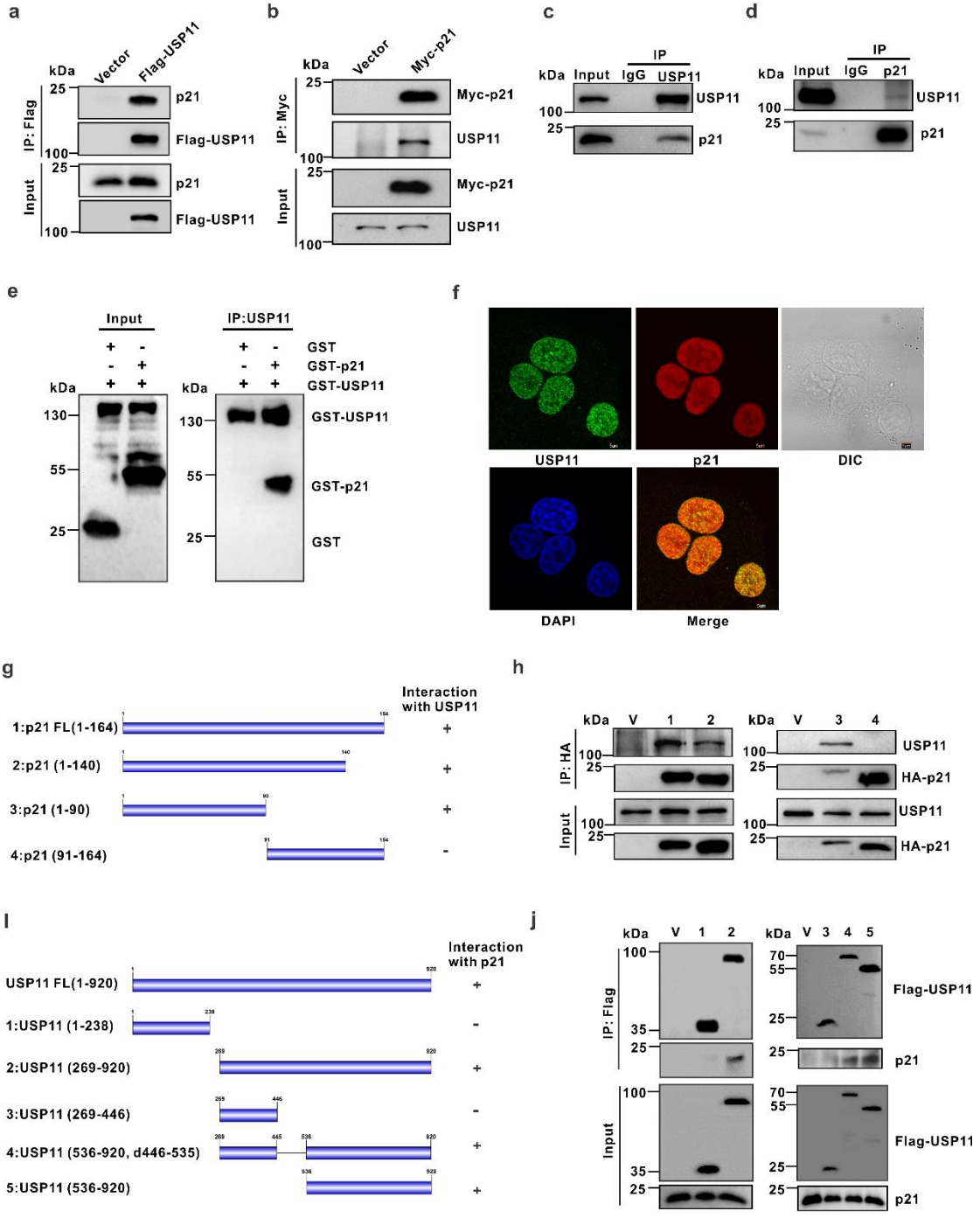

Figure 1 USP11 interacts with p21. (a and b) A549 cells were transfected with plasmids expressing either Flag-USP11 or Myc-p21. Total cell lysates were subjected to immunoprecipitation with anti-Flag (a) or anti-Myc antibody (b). The

immunoprecipitates were then probed with the indicated antibodies. (c and d) A549 cell lysates were subjected to immunoprecipitation with control IgG, anti-USP11(c) or anti-p21 (d) antibody. The immunopreciptates were then probed with the indicated antibodies. (e) GST, GST-p21 and GST-USP11 produced from bacteria were assessed using western blotting, and anti-USP11 antibodies were used to immobilize purified GST-USP11 protein onto protein A beads; these beads were then incubated with purified GST or GST-p21. The bound proteins were then eluted and analyzed by western blotting using anti-GST antibodies. (f) The subcellular localization of endogenous USP11 (green) and p21 (red) in A549 cells were visualized using immunofluorescence with anti-USP11 and anti-p21 antibodies. DNA was stained with DAPI, and a merged view of the red and green channels within the same field is shown (merge). (g) Schematic representation of the HA-tagged full-length p21 (FL) and its various deletion mutants. (h) HEK293 cells transfected with the indicated constructs were lysed. The cell lysates were subjected to immunoprecipitation with anti-HA antibodies, and the immunoprecipitates were then probed with the indicated antibodies. (V: Vector) (i) Schematic representation of the Flag-tagged full-length USP11 (FL) and its various deletion mutants. (j) A549 cells transfected with the indicated constructs were lysed. The cell lysates were subjected to immunoprecipitation with the anti-Flag antibodies, and the immunoprecipitates were then probed with the indicated antibodies. (V: Vector)

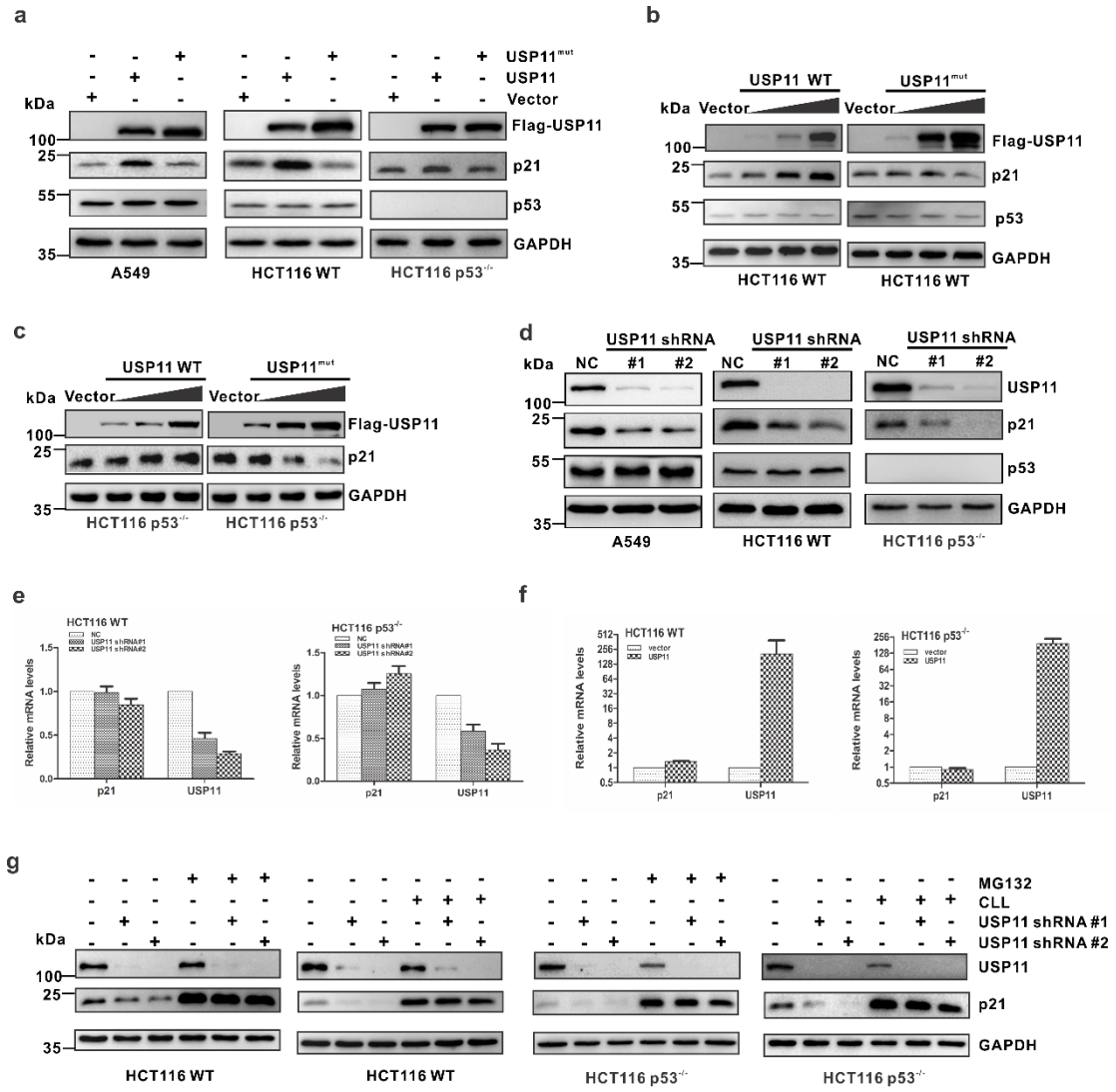

Figure 2 USP11 regulates the steady-state level of p21. (a) A549, HCT116 WT and HCT116 p53$^{-/-}$ cells were transfected with the indicated constructs. Total protein was extracted and subjected to western blotting using the indicated antibodies. (b and c) Increasing amounts of USP11 WT or USP11^{mut} were transfected into HCT116 WT (b) and HCT116 p53$^{-/-}$ (c) cells, and total protein was extracted from these cells and subjected to western blotting using the indicated antibodies. (d) A549, HCT116 WT and HCT116 p53$^{-/-}$ cells were infected with the indicated lentiviral constructs. The resulting cell extracts were analyzed using western blotting with the indicated antibodies. (e and

f) Total RNA from cells either infected with the indicated lentiviral shRNAs (d) or cells transfected with the indicated constructs (f) was isolated and subjected to qRT-PCR. The error bars represent the standard deviation (SD) of triplicate measurements. (g) HCT116 WT and HCT116 p53−/− cells infected with the indicated lentiviral shRNAs were treated with DMSO, MG132 (20 μM) or CLL (Clasto-Lactacystin β-lactone, 10 μM) for 6 h, and the indicated proteins were analyzed using western blotting.

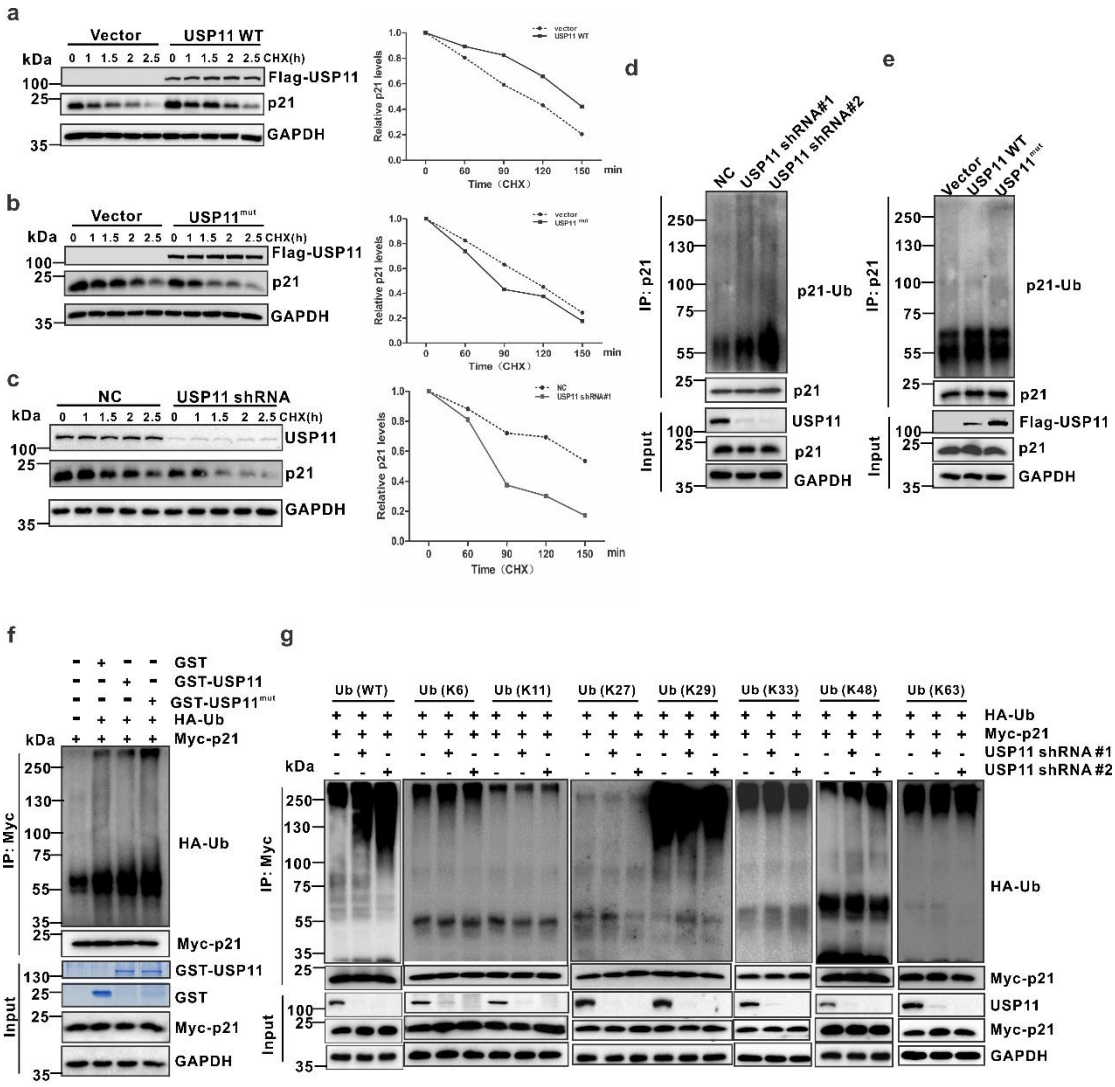

Figure 3 USP11 stabilizes p21 via deubiquitylation. (a and b) HCT116 WT cells transfected with the indicated constructs were treated with 50 μg ml^{-1} cycloheximide (CHX), collected at the indicated time points and immunoblotted with the indicated antibodies. Quantification of the p21 levels relative to GAPDH expression is shown. (c) HCT116 WT cells infected with the indicated lentiviral shRNAs, were treated with 50 μg ml^{-1} CHX, collected at different time points and then immunoblotted with the indicated antibodies. Quantification of the p21 levels relative to GAPDH expression is shown. (d and e) HCT116 WT cells either infected with the indicated lentiviral shRNAs

(d) or transfected with the indicated constructs (e) were treated with MG132 (20 μM) for 6 h prior to harvest. p21 was immunoprecipitated with an anti-p21 antibody, and the immunoprecipitates were probed with the indicated antibodies. (f) Ubiquitylated Myc-p21 was incubated with either GST-tagged USP11 WT or the GST-tagged USP11^{mut} purified from bacteria using glutathione agarose. After co-incubation, Myc-p21 was immunoprecipitated using an anti-Myc antibody, and the immunoprecipitates were probed using antibodies against HA and Myc. Recombinant GST-USP11 was purified from bacteria and analyzed using SDS-PAGE and Coomassie blue staining. (g) Myc-p21 and various HA-ubiquitin mutants were transfected into HCT116 cells infected with the indicated lentiviral shRNA for 24h. The cells were treated with 20 μM the proteasome inhibitor MG132 (Sigma) for 6 h. Myc-p21 was immunoprecipitated with an anti-myc antibody, and the immunoprecipitates were probed with the indicated antibodies.

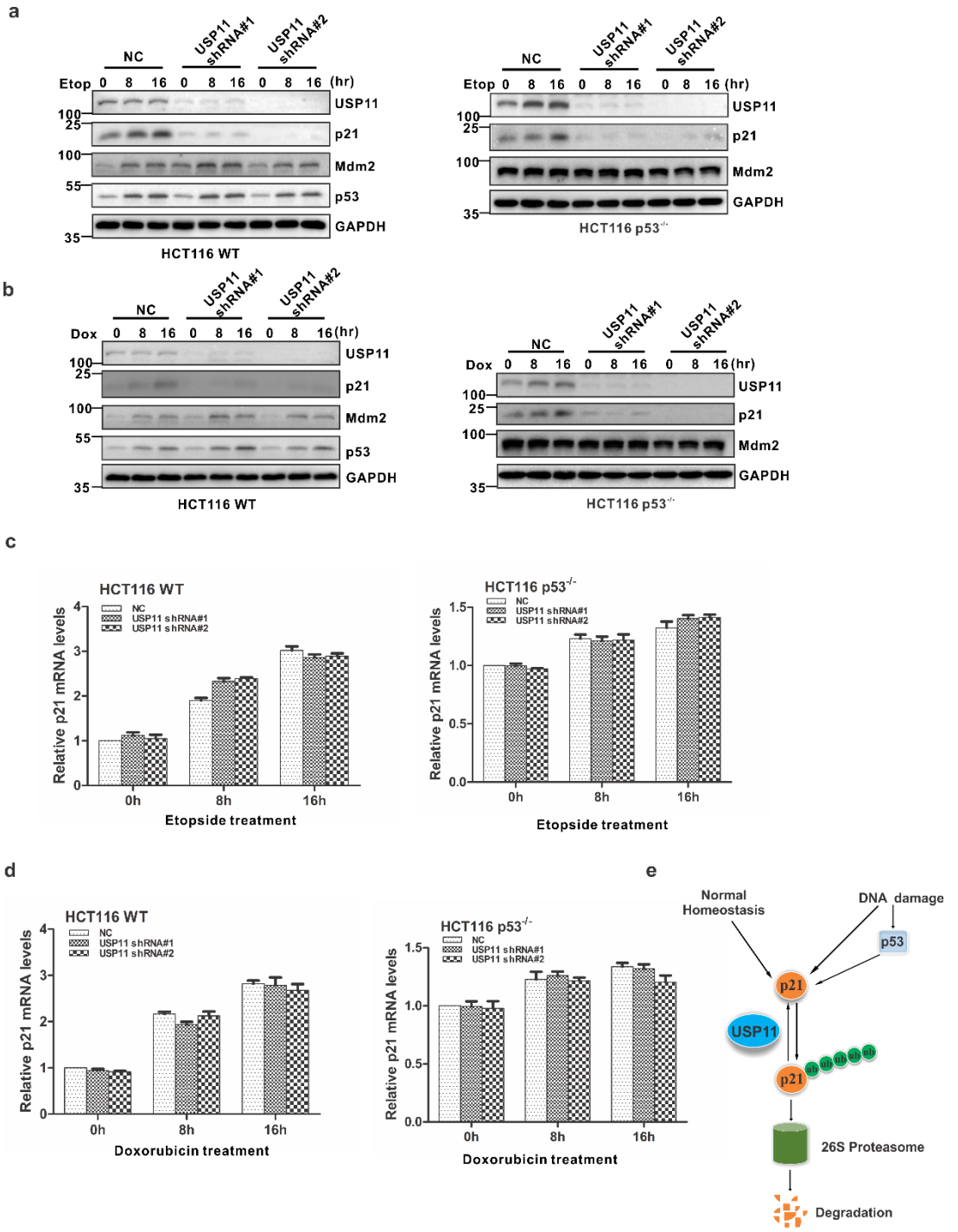

Figure 4 USP11 knockdown attenuates p21 elevation triggered by genotoxic agents.

(a and b) HCT116 WT **(a)** and HCT116 p53$^{-/-}$ **(b)** cells infected with the indicated lentiviral shRNAs were treated with 5 μM etoposide (Etop) or 0.2 μM doxorubicin (Dox) for either 8 or 16 h. Cell lysates were then extracted and subjected to western blotting.

(c and d) Total RNA from HCT116 WT (c) and HCT116 $p53^{-/-}$ (d) cells infected with the indicated lentiviral shRNAs and treated with 5 μM etoposide (Etop) or 0.2 μM doxorubicin (Dox) for either 8 or 16 h was isolated and subjected to qRT-PCR. The error bars represent the SD of triplicate measurements. (e) A proposed working model for p21 regulation by USP11 in response to DNA damage.

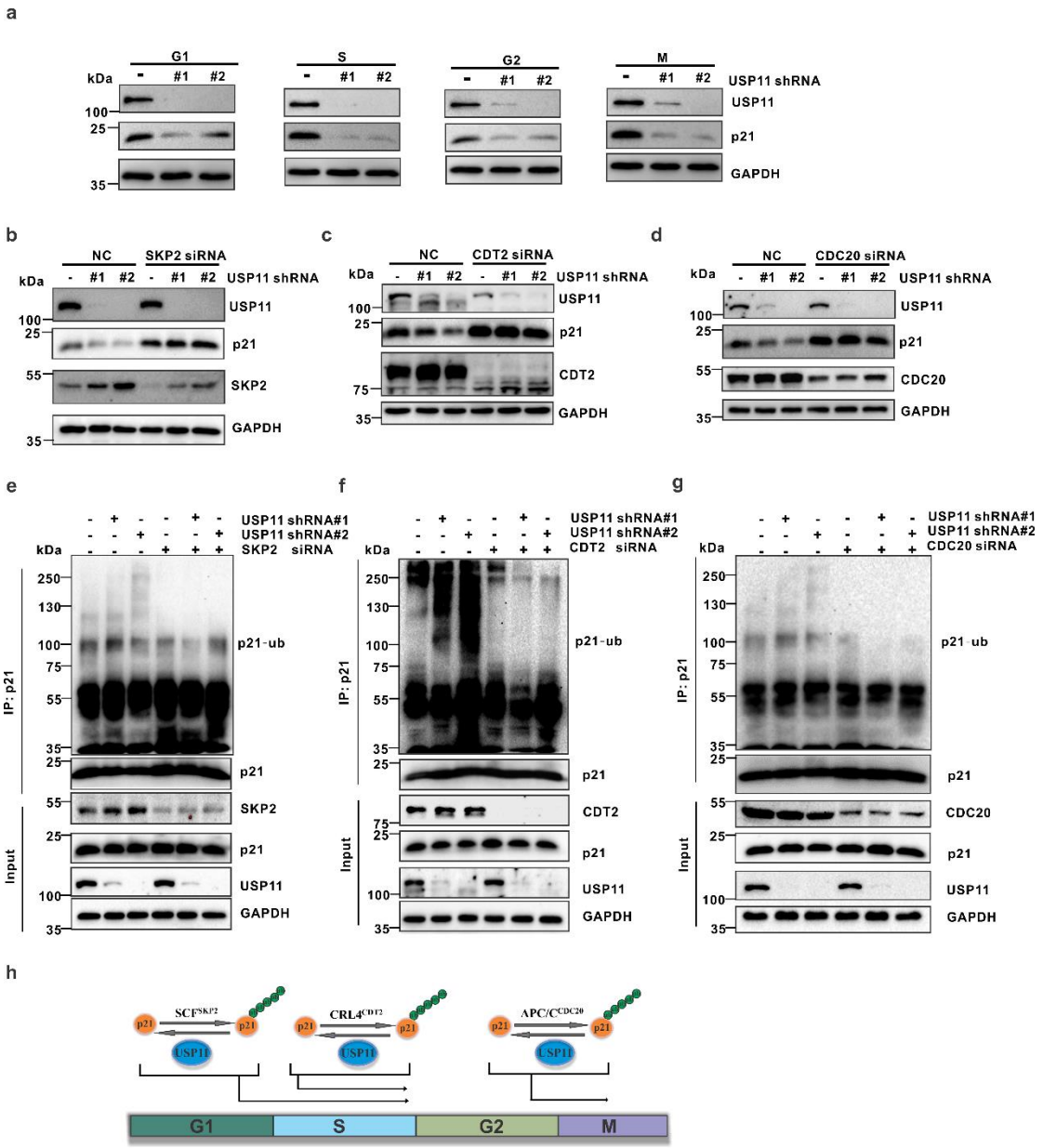

Figure 5 USP11 protects p21 from ubiquitin-mediated degradation. (a) HCT116 WT cells infected with the indicated lentiviral shRNAs were synchronized using a double thymidine block and released at the indicated phases. The resulting cell lysates were subjected to western blotting using the indicated antibodies. (b-d) HCT116 WT cells infected with the indicated shRNAs were transfected with scrambled, SKP2 (b), CDT2 (c), or CDC20 (d) siRNA for 48h, after which the cell lysates were harvested and

analyzed using western blotting. (e-g) HCT116 cells infected with the indicated shRNAs were transfected with scrambled, SKP2 (e), CDT2 (f) and CDC20 (g) as indicated for 48h and treated with 20 μM the proteasome inhibitor MG132 (Sigma) for another 6 h. p21 was immunoprecipitated with an anti-p21 antibody, and the immunoprecipitates were probed with the indicated antibodies. (h) A proposed working model that illustrates how USP11 reverse p21 ubiquitination in a cell-cycle independent manner

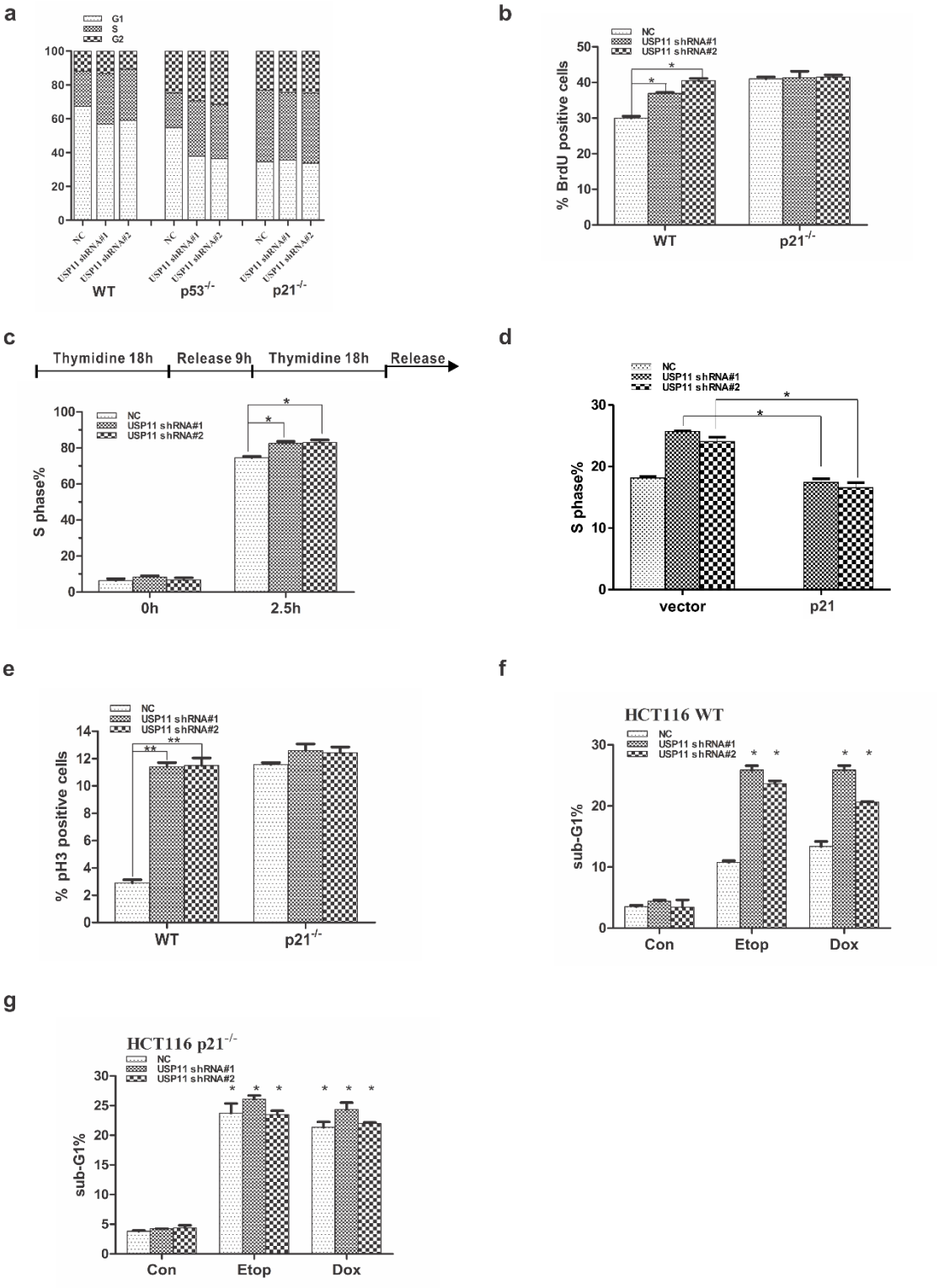

Figure 6 USP11 regulates the G1/S transition and DNA damage-induced G2 checkpoint in a p21-dependent manner. (a) HCT116 WT, HCT116 $p53^{-/-}$ and

HCT116 $p21^{-/-}$ cells infected with the indicated lentiviral shRNAs were stained with propidium iodide and analyzed using flow cytometry. (b) HCT116 WT and HCT116 $p21^{-/-}$ cells transfected with the indicated shRNAs were labeled with BrdU for 60 min before harvesting and then analyzed using flow cytometry. The error bars represent the mean ± SD of three independent experiments. *P <0.05. (C) HCT116 WT cells infected with the indicated lentiviral shRNAs were synchronized using a double thymidine block and release. The released cells were then harvested at the indicated times and analyzed using flow cytometry. The error bars represent the mean ± SD of three independent experiments. *P <0.05. (d) HCT116 WT cells infected with the indicated lentiviral shRNAs were transfected with the indicated constructs for 24 h. Cells were stained with propidium iodide and analyzed using flow cytometry. The error bars represent the mean ± SD of three independent experiments. *P <0.05. (e) HCT116 WT and HCT116 $p21^{-/-}$ cells infected the indicated lentiviral shRNAs were pretreated with 0.2 μM doxorubicin for 2 h, followed by synchronization with nocodazole (100 ng mL^{-1}) for 16 h. The mitotic index was determined using pH3 staining as a marker of mitosis. The error bars represent the mean±SD of three independent experiments. **P < 0.01. (f and g) HCT116 WT (f) and HCT116 $p21^{-/-}$ (g) cells were infected with the indicated lentiviral shRNAs, followed by treatment with either 0.2 μM doxorubicin (Dox) or 5 μM etoposide (Etop) for 48 h, and subsequent flow cytometry analysis of the sub-G1 fraction. The error bars indicate the mean±SD of three independent experiments. *P < 0.05.

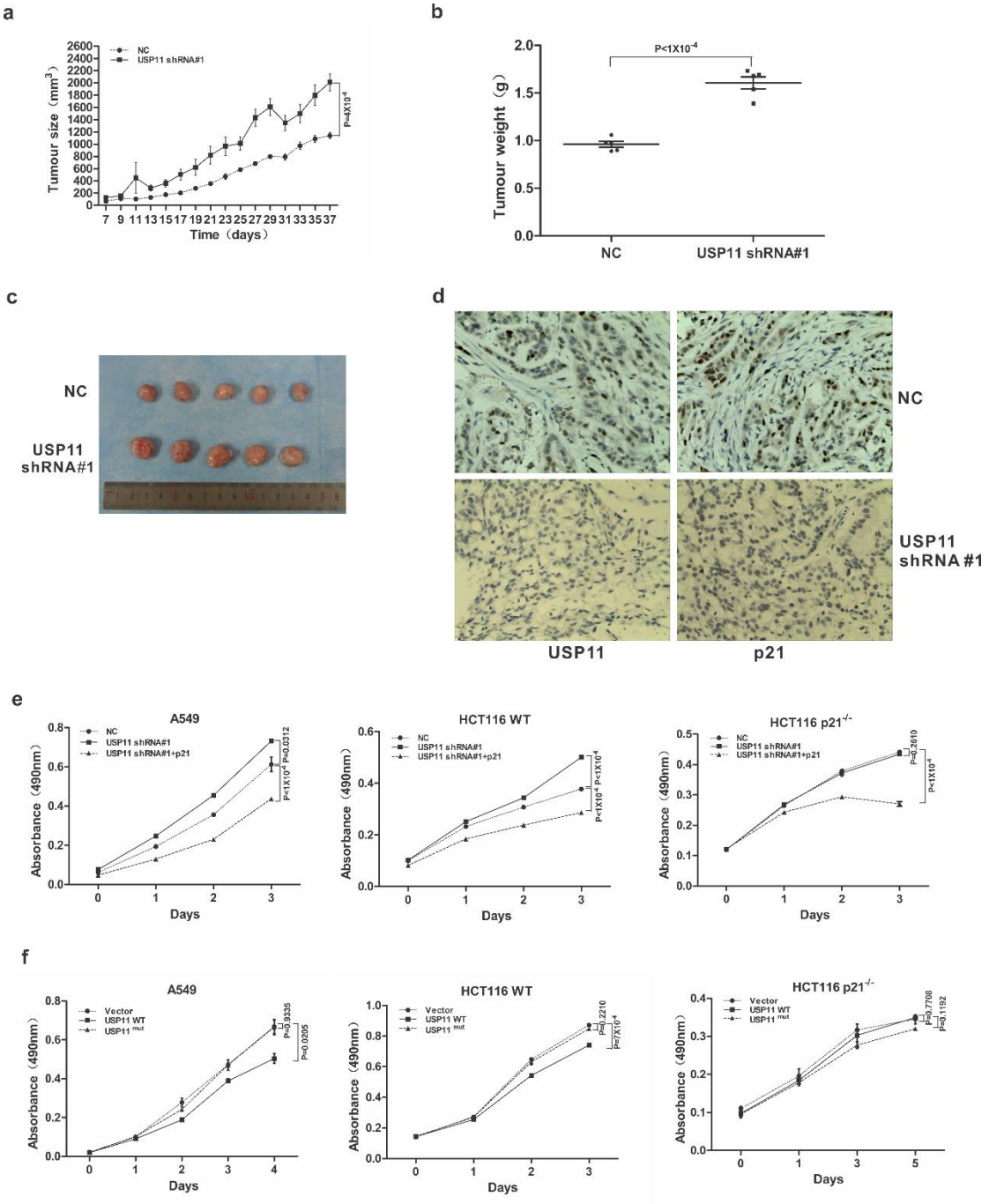

Figure 7 Loss of USP11 promotes tumor growth through the downregulation of p21. (a-c) Tumor growth of 5×10^6 A549 cells transfected with the indicated shRNAs and subcutaneously injected into mice. Tumor growth **(a)**, tumor weight **(b)** and tumor images **(c)** are shown. (d) Immunohistochemical analysis of USP11 and p21 expression in tumor xenografts. Formalin-fixed sections of tumors formed 37 days after injection

of A549 cells infected with the indicated lentiviral shRNAs were stained with anti-USP11 and anti-p21 antibodies. Typical fields of view are presented. (e) A549, HCT116 WT and HCT116 $p21^{-/-}$ cells were infected with the indicated lentiviral shRNAs, and then transfected with the indicated constructs. Cell proliferation was monitored using MTT assays at the indicated time points. Statistical significance was determined by a two-tailed, unpaired Student's t-test. (f) A549, HCT116 WT and HCT116 $p21^{-/-}$ cells were transfected with the indicated constructs, and cell proliferation was monitored using MTT assays at the indicated time points.